Electronic Supplementary Material (ESI) for Energy & Environmental Science.

Supplementary materials:

Broad temperature plateau for high ZTs in heavily doped p-type SnSe single crystals†

Kunling Peng,[a,b] Xu Lu,[a] Heng Zhan,[a] Si Hui,[c] Xiaodan Tang,[a,b] Guiwen Wang,[a,b] Jiyan Dai,[d] Ctirad Uher,[c] Guoyu Wang,[*b] Xiaoyuan Zhou.[*a]

[a.] *College of Physics, Chongqing University, Chongqing 401331, People's Republic of China.*

[b.] *Chongqing Institute of Green and Intelligent Technology, Chinese Academy of Sciences, Chongqing 400714, People's Republic of China.*

[c.] *Department of Physics, University of Michigan, Ann Arbor MI 48109, USA.*

[d.] *Department of Applied Physics, The Hong Kong Polytechnic University Kowloon, Hong Kong.*

X-ray diffraction patterns (XRD)

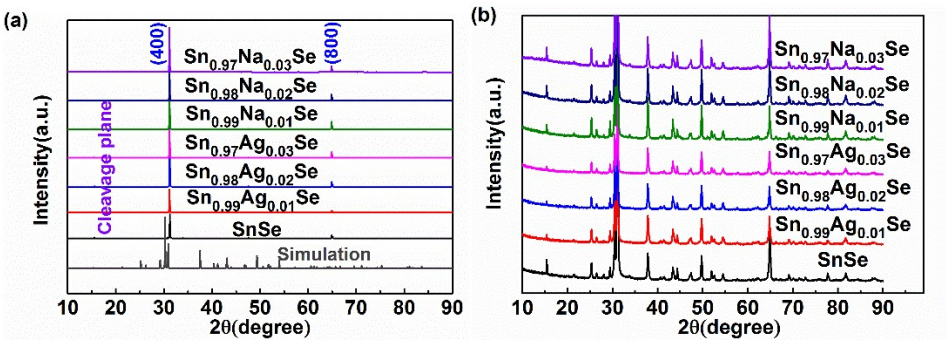

Figure S1a. XRD patterns of $Sn_{1-x}R_xSe$ (R=Ag, Na; x=0, 0.01, 0.02, 0.03) along the cleavage plane, and the simulated diffraction pattern. **Figure S1b.** X-ray diffraction patterns of $Sn_{1-x}R_xSe$ (R=Ag, Na; x=0, 0.01, 0.02, 0.03) powder.

Figure S1a displays the XRD patterns of $Sn_{1-x}R_xSe$ (R=Ag, Na; x=0, 0.01, 0.02, 0.03) single crystals along the cleavage plane. The (400) and (800) planes confirm that the $Sn_{1-x}R_xSe$ crystals are cleaved along the b-c plane. The as-prepared single crystals were then pulverized and X-ray diffraction characterization on an *X'Pert³ Powder (Panalytic)* using Cu Kα (λ=1.5418 Å) radiation was carried out as shown in Figure S1b, a pure SnSe phase with *Pnma* space group was obtained in our study. Lattice parameters as function of different contents of the dopant are shown in Table S1. The volume of the unit cell of doped crystals is slightly larger than that of the undoped crystal. Moreover, the cell volume of Ag-doped SnSe is larger than that of Na-doped crystals due to the fact that the radius of Ag^+ ions (1.26 Å) is larger than the radius of Na^+ ions (0.97 Å).

Table S1. Lattice parameters derived from the powder XRD patterns.

Sample	*a*(Å)	*b*(Å)	*c*(Å)	Volume(Å^3)
SnSe	11.4924	4.1513	4.4326	211.47
$Sn_{0.99}Ag_{0.01}Se$	11.4953	4.1494	4.4390	211.74
$Sn_{0.98}Ag_{0.02}Se$	11.4935	4.1501	4.4399	211.78
$Sn_{0.97}Ag_{0.03}Se$	11.4957	4.1508	4.4386	211.79
$Sn_{0.99}Na_{0.01}Se$	11.4969	4.1510	4.4322	211.52
$Sn_{0.98}Na_{0.02}Se$	11.4993	4.1465	4.4337	211.40
$Sn_{0.97}Na_{0.03}Se$	11.4975	4.1511	4.4352	211.70

The electronic transport properties

Table S2. Room temperature transport properties of $Sn_{1-x}R_xSe$ (R=Ag, Na; x=0, 0.01, 0.02, 0.03)

Sample	n_H (10^{17} cm^{-3})	σ (10^3 S/m)	Mobility (cm^2/Vs)	Seebeck (μV/K)	m^* (m_e)
SnSe	4.45	1.07	150.3	431	0.12
$Sn_{0.99}Ag_{0.01}Se$	26.9	6.15	142.9	284	0.26
$Sn_{0.98}Ag_{0.02}Se$	71.5	16.1	139.8	237	0.42
$Sn_{0.97}Ag_{0.03}Se$	127	25.5	125.5	233	0.61
$Sn_{0.99}Na_{0.01}Se$	226	48.6	134.4	212	0.82
$Sn_{0.98}Na_{0.02}Se$	477	73.5	96.3	172	1.09
$Sn_{0.97}Na_{0.03}Se$	822	109	82.9	160	1.45

Room-temperature Hall coefficients were measured via a home-made apparatus in the applied field of ±1 T. The band structure (see the main text in Figure 3) confirms the estimated values of effective mass calculated from the Seebeck coefficient at room temperature. The carrier concentration, carrier mobility and effective mass are roughly estimated by the single band model.

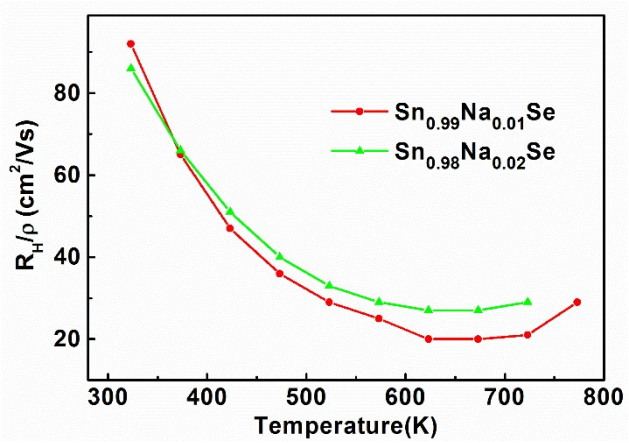

Figure S2. R_H/ρ for $Sn_{0.99}Na_{0.01}Se$ and $Sn_{0.98}Na_{0.02}Se$ crystals.

The thermal transport properties

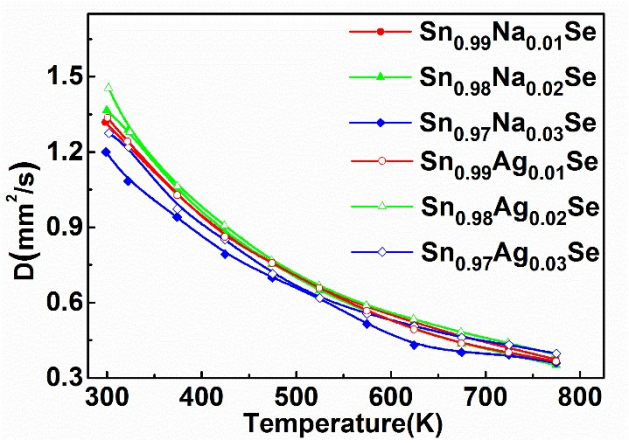

Figure S3. Thermal diffusivity as a function of temperature for $Sn_{1-x}R_xSe$ (R=Ag, Na; x=0.01, 0.02, 0.03)

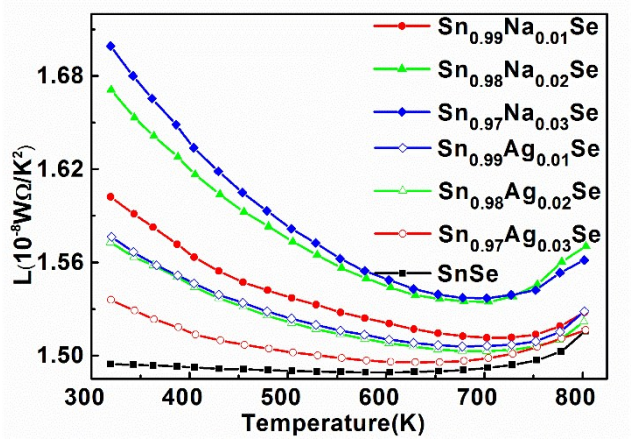

Figure S4. The Lorenz number as a function of temperature for $Sn_{1-x}R_xSe$ (R=Ag, Na; x=0, 0.01, 0.02, 0.03), and the scattering factor r = -1/2

The Lorenz number depends on the degree of elasticity in carrier scattering, is defined as[S1]

$$L = \left(\frac{k_B}{q}\right)^2 \left[\frac{\left(r+\frac{7}{2}\right)F_{r+\frac{5}{2}}(\eta)}{\left(r+\frac{5}{2}\right)F_{r+\frac{1}{2}}(\eta)} - \left(\frac{\left(r+\frac{5}{2}\right)F_{r+\frac{3}{2}}(\eta)}{\left(r+\frac{3}{2}\right)F_{r+\frac{1}{2}}(\eta)}\right)^2\right] \quad \text{(S1)}$$

with the Fermi integral

$$F_n(\eta) = \int_0^\infty \frac{\xi^n}{1+e^{\xi-\eta}} d\xi \quad \text{(S2)}$$

where r is the scattering factor, which gives the exponent of the energy dependence on the charge carrier mean free path, η is the reduced Fermi energy from the Seebeck coefficient given by equation (S3).

(S3)

$$S = \mp \frac{k_B}{q}\left(\eta - \frac{\left(r+\frac{5}{2}\right)F_{r+\frac{3}{2}}(\eta)}{\left(r+\frac{3}{2}\right)F_{r+\frac{1}{2}}(\eta)}\right)$$

The thermal stability

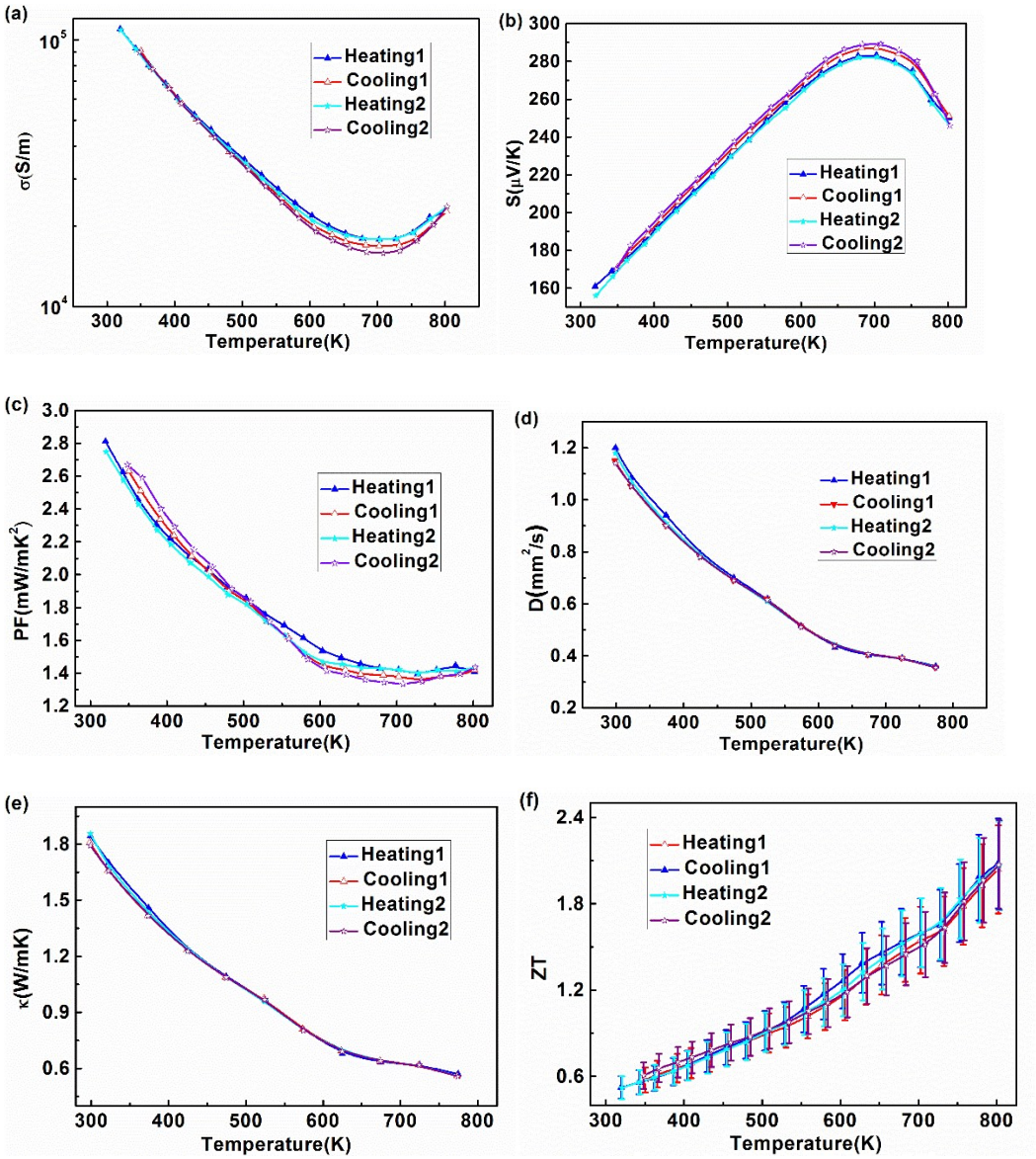

Figure S5. The TE performance of $Sn_{0.97}Na_{0.03}Se$ single crystals during two heating-cooling cycle, indicating a very good thermal stability for the doped SnSe single

crystal.

Supplementary References

S1. T. Dahal, Q. Jie, Y. C. Lan, C. F. Guo and Z. F. Ren, *Phys Chem Chem Phys*, 2014, **16**, 18170-18175.